Korean J. Chem. Eng., 37(4), 670-676 (2020)
DOI: 10.1007/s11814-020-0491-8

pISSN: 0256-1115
eISSN: 1975-7220

Microwave-assisted production of biodiesel using metal-organic framework $Mg_3(bdc)_3(H_2O)_2$

Howaida AbdelSalam*, Heba Hassan El-Maghrbi,†, Fouad Zahran***,†, and Tamer Zaki**,****

*Analysis and Evaluation Division, Egyptian Petroleum Research Institute, Nasr City, P. O. Box 11727, Cairo, Egypt
**Catalysis Department, Petroleum Refining Division, Egyptian Petroleum Research Institute, Nasr City, P. O. Box 11727, Cairo, Egypt
***Chemistry Department, Faculty of Science, Helwan University, 11795, Cairo, Egypt
****EPRI-Nanotechnology Center, Egyptian Petroleum Research Institute, Nasr City, P. O. Box 11727, Cairo, Egypt
(*Received 24 September 2019 • accepted 12 January 2020*)

Abstract−Metal-organic framework Mg-MOF: ($Mg_3(bdc)_3(H_2O)_2$) was synthesized via microwave (MW) irradiation, then used in the microwave-assisted production of biodiesel from oleic acid. Microwave irradiation was used as an alternative ecofriendly route to conventional heating. The synthesized Mg-MOF sample was characterized by XRD, TGA, FT-IR, nitrogen adsorption/desorption and TEM techniques. The catalytic activity of Mg-MOF in the microwave-assisted production of Biodiesel from oleic acid and methanol was studied. Vacancies created upon removal of linkers, metal clusters composed MOF frameworks, small pore size and its surface area are responsible for the high catalytic activity of the prepared Mg-MOF. The results indicated that Mg-MOF catalyst showed high conversion percentage (97%) that followed pseudo-first order, under mild reaction conditions (MW power: 150 watts, reaction time: 8 min, molar ratio of oleic acid to methanol: 1 : 15 and catalyst amount 0.15 wt%).

Keywords: Microwave-assisted Production, MOF, Esterification, Heterogeneous Catalysis, Biodiesel

INTRODUCTION

Diesel is fuel used in heavy duty machines and it could be petrodiesel or biodiesel. Biodiesel is mono alkyl ester with high molecular weight delivered from vegetables or animal fats [1]. As a global trend and need, all petroleum fuels are being replaced with ecofriendly and renewable sources not only because of rising costs and depletion of petroleum, but also because renewable sources have good advantages [2,3]. Biodiesel has become one the most common renewable fuels and it has high lubricity in comparison with low sulfur content diesel, which could increase engine life; it also has higher flash point value, 135 °C, more than double that of low sulfur content diesel [4].

Biodiesel is produced by homogeneous or heterogeneous catalytic esterification and trans-esterification reactions of vegetable oil or animal fats with low molecular weight alcohol biologically or chemically. Biodiesel can be produced biologically using fungi, yeasts and bacteria, those belonging to Ryzophus, Rhizomucor and Candida family. The main disadvantages of the biological route arise from the origin of the catalyst used in the reactions where enzymes have low reaction rate, high cost and low reusability [5-8]. On the other hand, biodiesel is produced chemically via traditional catalytic reactions. The widespread catalysts used in the production of biodiesel chemically are the homogeneous catalysts, such as base catalysts (NaOH and KOH) and acid catalysts (H_2SO_4 or HCl) [9]. Homogeneous catalysts have many advantages like being highly effective for acceleration reaction [10]. However, the disadvantages of the homogeneous catalysts include soap formation, corrosion of the reactor, unavailability of reusing and successively increasing the cost of productions [11].

Metal-organic frameworks (MOFs) are good heterogeneous catalysts. Heterogeneous catalysts are more environmentally friendly, non-corrosive and can be reused [12]. Many works had been done in the fields of esterification and transesterification reactions using heterogeneous acid catalysts [11,13-15]. MOFs constructed from inorganic cation with organic linkers offer tremendous possibilities for the catalytic application due to unique features, such as high porosity, surface area, and the ability for tailoring design for tuning the acidity/basicity properties [12]. Within the reported MOFs, Mg-based metal-organic frameworks are distinguished with being lightweight and having fewer toxicity properties [16-22]. Functionalized Mg-MOFs: MIL-101(Cr), MIL-53(Fe) and MIL-100(Fe) are considered as competitive catalyst for acid-catalyzed esterification process [12,23-25].

Microwave-assisted technology is a promising methodology that has revolutionized chemical synthesis and discovery. The main advantages of the microwave irradiation route in comparison with conventional methods are low energy consumption, ecofriendliness, short processing time and high reaction rates [26-29]. Recent studies on microwave-assisted production of biodiesel from different sources show the high potential of microwave technology to produce high biodiesel yield with low energy consumption [30-34].

Oleic acid is the most common monounsaturated fatty acid that

†To whom correspondence should be addressed.
E-mail: helmaghrbi@gmail.com, f.zahran@gmail.com, Fouad_zahran@science.helwan.edu.eg

can be found in both animal fats and vegetable oils and it is widely used to produce biodiesel [23,35-39]. Methanol is a commercially well known and cheap low molecular weight alcohol. Oleic acid and methanol were chosen as candidates for microwave-assisted production of biodiesel.

To the best of our knowledge, microwave-assisted biodiesel production using magnesium based MOF (Mg-MOF) has not been evaluated before. In the present work, microwave-assisted technology was used to prepare Mg-MOF, ($Mg_3(bdc)_3(H_2O)_2$). Then, the prepared MOF was utilized in the biodiesel production through the esterification of oleic acid with methanol via microwave irradiation too.

EXPERIMENTAL

1. Materials

Mg(II) nitrate hexahydrate (>99%), 1,4-benzenedicarboxylic acid (98%), *N*,*N*-dimethylformamide (>99.8%), ethanol (99.5%), oleic acid (>98% w/w) and methanol (>99.8%) were supplied from Sigma-Aldrich andwere used without any purification. Deionized water was used in in all experiments.

2. Characterizations of Materials

Thermogravimetric analysis (TGA, TA Instruments) proceeded with a heating rate of 10 °C/min in a nitrogen atmosphere. The powder XRD data was accomplished with a PAN analytical X'PERT PRO using CuKα X-ray radiation (λ=1.540 Å) to investigate the crystal structure of the sample. The specific surface area of the prepared nanocomposite and its pore volume were measured from the N_2 adsorption-desorption isotherms at liquid nitrogen temperature using surface area and porosity analyzer (Micromeritics ASAP 2020). Before measurement, the sample was degassed at 150 °C under vacuum. Fourier-transform infrared spectroscopy (FT-IR) spectrum of the sample was registered on Perkin Elmer (model spectrum one FT-IR spectrometer, USA) using KBr pellets over wave number range between 4,000 and 500 cm^{-1}. The morphology of the prepared sample was characterized by transmission electron microscope (TEM) JEOL 2100-lab6.

3. Microwave-assisted Synthesis of $Mg_3(bdc)_3(H_2O)_2$

The precursor salts, H_2BDC (4.06 mmol) and $Mg(NO_3)_2{\cdot}6H_2O$ (1.85 mmol), were dissolved in a mixture of ethanol, deionized water and DMF in a molar ratio (1 : 3 : 11), using ultrasonic waves. The homogeneous solution was transferred to a round flask connected with a reflux condenser and placed in microwave oven at power 300 watts for three hours. The sample was then cooled to room temperature. The product had been washed using methanol for two times, and then it was immersed in 10 ml methanol for two days. Finally, the trapped solvent's molecules in the structure of the as-synthesized sample were desorbed at 220 °C under the vacuum condition.

4. Microwave-assisted Production of Biodiesel

Microwave-assisted esterification of oleic acid with methanol using the prepared Mg-MOF, $Mg_3(bdc)_3(H_2O)_2$, was carried out in a 100 mL round flask equipped with a mechanical stirrer inside the microwave. An appropriate amount of the Mg-MOF catalyst was added stepwise to the mixture of fatty acid and alcohol. The reaction was achieved under microwave irradiation within different times. At the end of the reactions, the Mg-MOF catalyst was filtrated away. Conversion percent of oleic acid to the methyl oleate was determined by measuring the acidity of the product via the titration against 0.1 M Na(OH) in the presence of phenolphthalein as an indicator. The recovered catalyst was washed thoroughly and then dried.

RESULTS AND DISCUSSION

1. Characterization of Mg-MOF

Phases present in the prepared Mg-MOF catalyst were investigated in view of X-ray diffraction pattern (Fig. 1). XRD pattern obtained was in agreement with the simulated pattern of the $Mg_3(bdc)_3(H_2O)_2$ framework [18]. All characteristic peaks appearing in the simulated pattern can be easily located in the prepared sample.

The curve of the thermogravimetric analysis (TGA) of the as-synthesized Mg-MOF exhibited two weight loss steps (Fig. 2). The first weight loss (17.7 wt%) was achieved during raising the temperature from 30 °C to 208 °C, and the second weight loss occurred

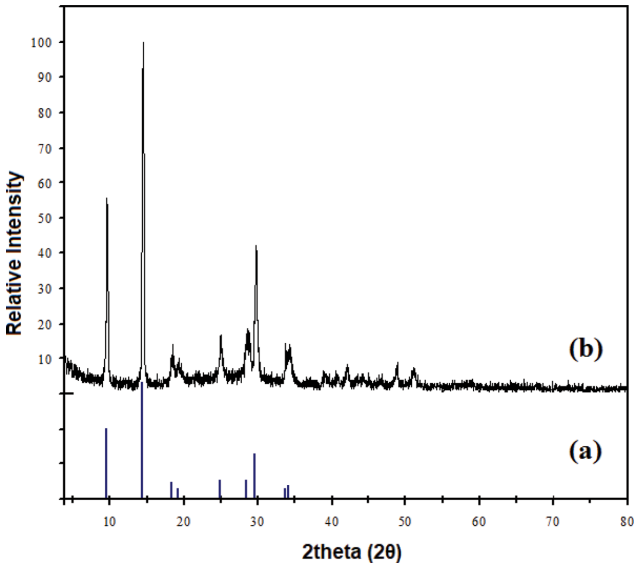

Fig. 1. (a) Simulated powder X-ray diffraction (PXRD) pattern for $Mg_3(bdc)_3(H_2O)_2$ [18]; (b) experimental PXRD pattern of the synthesized sample.

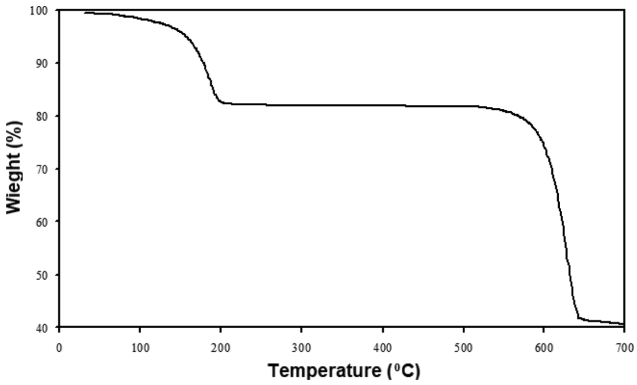

Fig. 2. TGA trace of as-synthesized Mg-MOF sample.

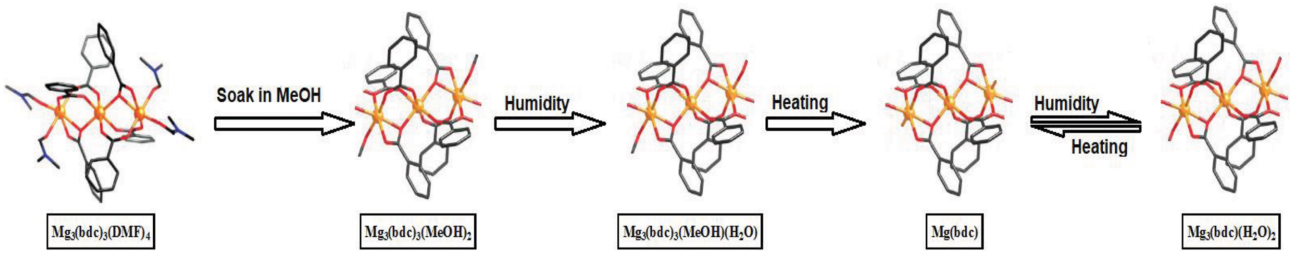

Scheme 1. Transformation ($Mg_3(bdc)_3(DMF)_4$) to ($Mg_3(bdc)_3(H_2O)_2$) [18]. Orange (magnesium); red (oxygen); grey (carbon); blue (nitrogen).

above 520 °C (~41.3 wt%). The value of the first weight loss (17.7 wt%) was between the calculated weight loss resulting from the desorption of two moles of methanol (21.3 wt%), and the calculated weight loss resulted from the desorption of two moles of water (13.2 wt%).

Also, the weight of the remaining ash could be attributed to the formation of three moles of MgO (calc. 41.5 wt%).

The results of powder X-ray diffraction and thermogravimetric analyses after and before the thermal treatment, successively, clarified that the 2D metal-organic framework of formula $Mg_3(bdc)_3(DMF)_4$ had been prepared in the first stage of synthesis method. However, due to the long time of soaking of the as-synthesized sample in methanol (two days), the DMF molecules that coordinated to the terminal magnesium ions and occupied the space in-between the layers of $Mg_3(bdc)_3$ were replaced by the methanol molecules.

Due to the volatile nature of the methanol species and its weak bond with magnesium ions, the partial replacement of methanol molecules by the water molecules, which is supplied from the surrounding environment, was achieved (Scheme 1) [18]. FTIR, TGA and XRD for MOF before and after immersing in methanol are discussed in detail in the supplementary file.

It can be noticed in the value of the first weight loss (Fig. 2). Accordingly, the formula of the as-synthesized sample could be $(Mg_3(bdc)_3(MeOH)(H_2O)$; the calculated first weight loss=17.4 wt%. Due to the hygroscopic nature of the MOF [18], after the heating process at 220 °C under vacuum conditions and then the exposing to the surrounded environment, the methanol molecules were entirely replaced with the water molecules ($Mg_3(bdc)_3(H_2O)_2$), which can be shown in the XRD pattern of the thermally treated sample (Fig. 1).

The FTIR spectrum of as-synthesized $Mg_3(bdc)_3(H_2O)_2$ (Fig. 3) shows the vibration bands at ~3,450 and ~3,114 cm^{-1}, due to the coordinated water molecules in the structure of framework and two peaks at 1,587 and 1,385 cm^{-1} corresponding to the symmetric and asymmetric (COO^-). Many small peaks are observed in the range of 1,250 to 1,010 cm^{-1}. These peaks are attributed to the vibration of C-H groups of the linker [40]. The band near 700 cm^{-1} may be ascribed to in-plane and out-of-plane bending modes of (COO^-) group. Also, the spectrum clarified peak occurred at 510 cm^{-1}, which specified the vibration of Mg-O [41].

The nitrogen adsorption isotherm of the magnesium framework exhibits type II profile (Fig. 4). However, the isotherm shows a hysteresis, which may indicate the formation of few mesopores,

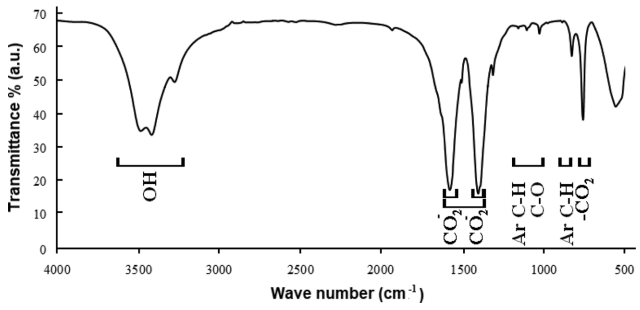

Fig. 3. The FT-IR spectrum of the synthesized Mg-MOF sample.

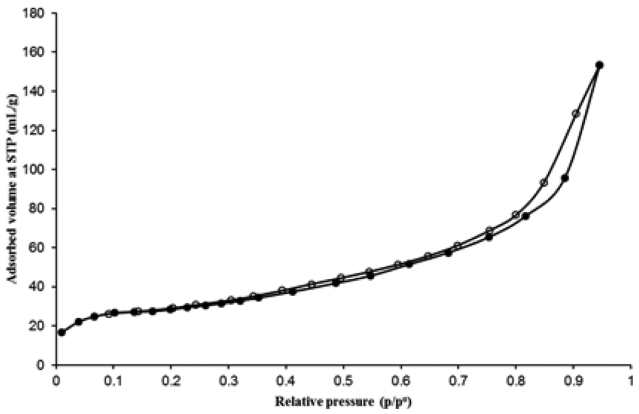

Fig. 4. Nitrogen adsorption-desorption isotherm of as-synthesized Mg-MOF sample.

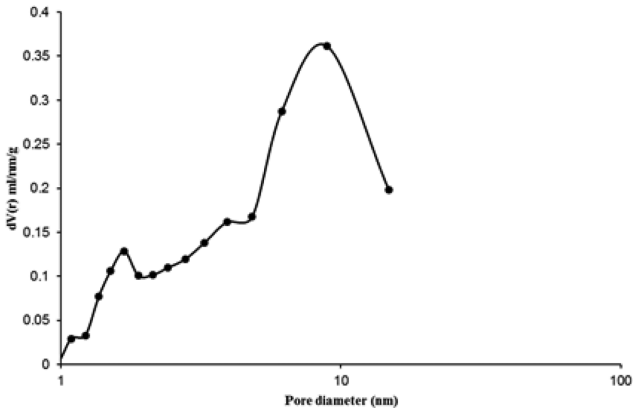

Fig. 5. Pore size distributions of as-synthesized Mg-MOF sample.

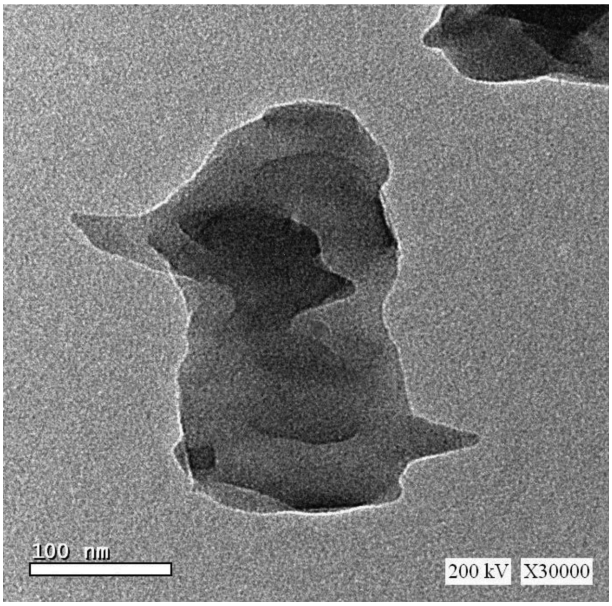

Fig. 6. TEM image of as-synthesized Mg-MOF sample.

resulting from the partial breakage of some metal-ligand bonds during the heating at 220 °C. Accordingly, the determined BET surface area was 162 m^2/g. The presence of the mesopores within the structure of the prepared MOF can be noticed in the pore size distributions represented in Fig. 5.

The TEM image (Fig. 6) of the prepared catalyst shows that Mg-based MOF is a transparent sheet with dimension (~150-250 nm) and thickness of less than 100 nm.

2. Microwave-assisted Production of Biodiesel from Oleic Acid

A control experiment was achieved in the absence of Mg-MOF. The results showed negligible conversion under microwave irradiation of power 100 watts for 10 min and oleic acid to methanol molar ratio, 1 : 10.

The Lewis acid character of the metal organic framework arises from vacancies created upon removal of linker solvent molecules. Since highly volatile methanol was used, this could explain the high catalytic activity of the resulting defective framework Mg-MOF. In general, catalytic activity increases with the number of missing linkers. In addition to vacancies created upon removal of linkers, metal clusters of composed MOF frameworks may be another source of intrinsic Brønsted acidity. The small dimension of the prepared Mg-MOF nanosheets (Fig. 6) and its surface area (162 m^2/g) have a good influence also on its catalytic activity.

Fig. 7(a) shows a gradual increase in the oleic acid conversion from 19.6 to ~100% with increasing the reaction time from 1 to 10 min, respectively, using 0.15 wt% Mg-MOF catalyst under microwave irradiation of power 100 watts and oleic acid to methanol molar ratio of 1 : 10. This high activity within relatively short reaction time could be attributed to the well known functional influence of the microwave irradiation in reducing the reaction time [12].

The kinetics of the esterification reaction of oleic acid with methanol over Mg-MOF was correlated with the pseudo-first-order model due to the high concentration of methanol. Since methanol was taken in large excess (oleic acid to methanol molar ratio, 1 : 10), it

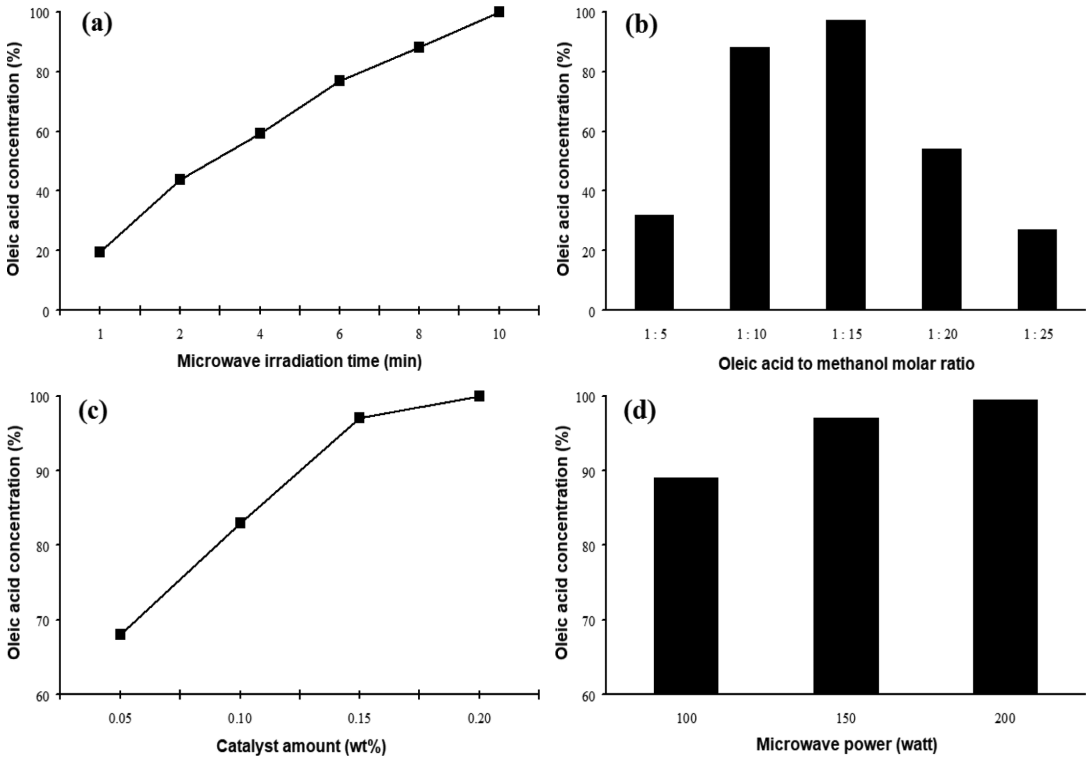

Fig. 7. Conversion of oleic acid with methanol, using Mg-MOF under MW irradiation: (a) Effect of reaction time; (b) effect of oleic acid with methanol molar ratio; (c) effect of catalyst amount; and (d) effect of microwave power.

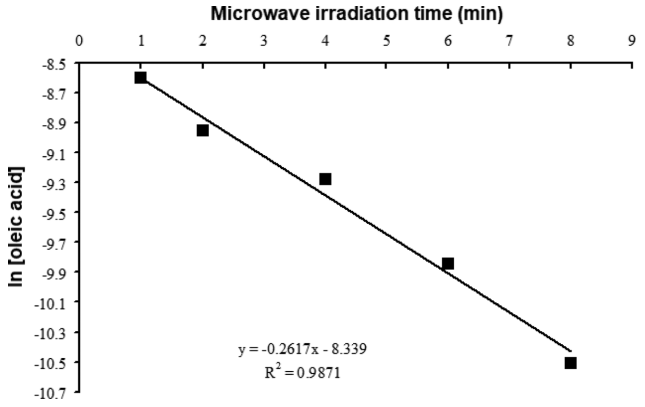

Fig. 8. Arrhenius plot of oleic acid concentration as function of time.

was expected that the rate law followed pseudo-first-order. The kinetic relation between the concentration of the remained oleic acid and the related reaction time was calculated according to the equation ($\ln [\text{oleic acid}]_t = -kt + \ln [\text{oleic acid}]_0$), whereas $[\text{oleic acid}]_t$ is the concentration of the remained oleic acid at time t (min), k (mol/mL·min) is the rate constant and $[\text{oleic acid}]_0$ is the initial concentration of the oleic acid [42]. The plot of ln ($[\text{oleic acid}]_t$) versus time (Fig. 8) shows the linear relationship of oleic acid conversion concerning time (regression coefficient (R^2) was about 0.9871). The values of rate constant (k) and the half-life time ($t_{1/2} = k/0.693$); were 0.2617 mol/mL·min and 2.65 min, respectively.

The value for $t_{1/2}$ shows that the half-life depended solely on the reaction rate constant, (k). This observation indicates that esterification of oleic acid on this catalyst follows pseudo-first order, which was suggested by other researchers [42,43].

Molar ratio between oleic acid and the low molecular weight alcohol is one of the dynamic factors that affect the esterification process. Fig. 7(b) illustrates that the conversion of oleic acid increased sharply, from 32% to 97%, when molar ratio between fatty acid and alcohol increased from 1 : 5 to 1 : 15, using 0.15 wt% Mg-MOF catalyst under MW irradiation of power 100 watts for 8 min. However, increasing this molar ratio up to 1 : 25, the conversion of oleic acid decreased dramatically to 27%. It is well known that in case of base catalyst, the reactants diffuse to the active sites as an initial step. Then, the solid base catalyzes the esterification reaction via the alkoxide ion that was formed on the base sites (Scheme 2). Subsequently, the oleic acid initiates an electrophilic attack to the methanol molecule. After that, methyl oleate and water molecules are formed and effused [44].

Accordingly, the decrease of the conversion, upon the increase in the molar ratio of oleic acid to methanol, could be attributed to the blockage of the active metal sites on the catalyst surface by the excess alcohol that impeded the conversion reaction [25]. Also, the dilution of oleic acid by excess alcohol could be considered as a reason for the decrease of conversion. In addition, excess methanol molecules compete with oleic acid molecules for active sites that decreases the probability of oleic acid molecules to react at Mg-MOF surface [45].

Fig. 7(c) indicates that the esterification of oleic acid increased from 68 to ~100% with the increase in the catalyst amount from 0.05 wt% to 0.20 wt%, using oleic acid to methanol molar ratio, 1 : 15 under MW irradiation of power 100 watts for 8 min. This attitude may be attributed to the increase in the number of active base sites as the amount of Mg-MOF increased.

Fig. 7(d) clarifies that increasing the microwave power, under which the reaction was achieved, from 100 to 150 watts, resulted in

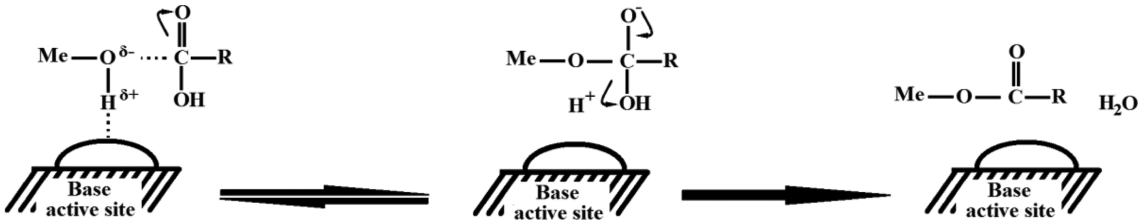

Scheme 2. Mechanism of esterification reaction in the presence of Mg-MOF.

Table 1. Comparison of esterification of oleic acid with methanol by Mg-MOF against different MOFs reported previously

Catalyst	Oleic acid : methanol molar ratio	Time (h)	Temp. (°C)	Catalyst (wt%)	Conversion (%)	Source of power	Ref.
UiO-66	1 : 26	2.00	60	49.19	83.0	Conventional	[49]
UiO-66-NH_2	1 : 26	2.00	60	49.19	93.0	Conventional	[49]
Sulfonic acid-functionalized MIL-101(Cr)	1 : 78	0.33	120	1.13	93.0	Microwave	[23]
NH2-MIL-101(Cr)-Sal-Zr	1 : 10	4.00	67	4.00	74.8	Conventional	[25]
Co-MOF	1 : 70	12.00	60	0.28	80.0	Ultrasonic	[50]
MIL-101(Cr)@2-Mercaptobenzimidazole ILs	1 : 10	4.00	67	11.00	91.0	Conventional	[51]
Sulfonated ILs functionalized UiO-66-2COOH	1 : 35	6.00	110	10.00	95.8	Conventional	[52]
Mg-MOF	1 : 15	0.13	65	0.15	97.0	Microwave	This work

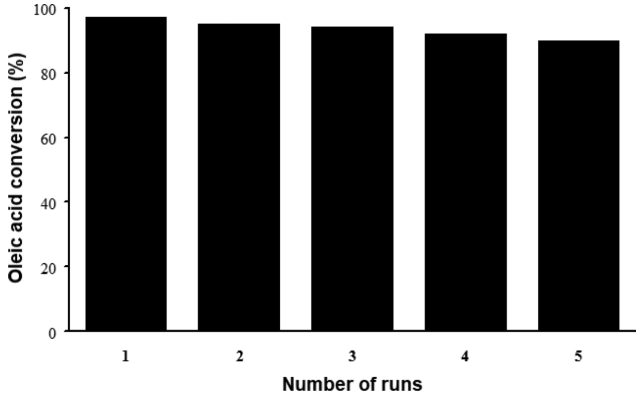

Fig. 9. Investigation of Mg-MOF reusability in the esterification reaction.

a noticeable increase in the oleic acid conversion from 89 to 97%, using 0.15 wt% Mg-MOF catalyst under MW irradiation for 8 min and oleic acid to methanol molar ratio, 1 : 15. However, when the microwave power increased to 200 watts, the oleic acid conversion was slightly increased to ~100%. Such behavior arises from increasing kinetic energy of reactants that results in an increase in the reaction rate. Also, the high temperature facilitates diffusion of reactant molecules into each other adsorption, which leads to higher catalytic efficiency [46].

It has been reported that the heating step after the synthesis process leads to partial decomposition of the bridging carboxylates the framework linker and formation of vacancy sites. These sites can be considered as active adsorption and catalytic sites [22]. Also, the removing of the coordinated DMF molecules could lead to the formation of active metal sites, which are favorable for the adsorption and catalytic processes [41,47]. In addition, the Mg-metal sites in MOFs structure are distinguished with its alkalinity nature, which favors the alkaline hydrolytic mechanism towards oleic acid and methanol [48].

Furthermore, Table 1 illustrates the esterification of oleic acid by methanol using different types of MOFs at their optimum experimental conditions that had been listed in the previous literature with the present work. It is well apparent that using Mg-MOF under microwave irradiation optimized the oil to methanol molar ratio, the catalyst to feed weight percentage, the reaction time and consumable power [23,25,49-52].

The reaction was carried out under conventional heat at (temperature: 70 °C, reaction time: 3 h, molar ratio of oleic acid to methanol: 1 : 15 and catalyst amount 0.15 wt%). The result indicates that Mg-MOF catalyst showed conversion percentage (83%) that was (97%) in case of microwave-assisted reaction. The result emphasizes the advantage of the microwave-assisted route.

The constancy of the Mg-MOF was studied by recovering catalyst for five cycles (Fig. 9) and achieving the XRD pattern of the catalyst after the fifth cycle (Fig. 10). Despite the apparent structural stability after five reusing cycles (Fig. 10), it is evident that measurable changes in the oleic acid conversion, from 97% to 92%, had occurred following the recovery of the catalyst after the fourth run. These changes are comparable with the previously published reports for the different MOFs as catalysts for oleic acid esterification [12,

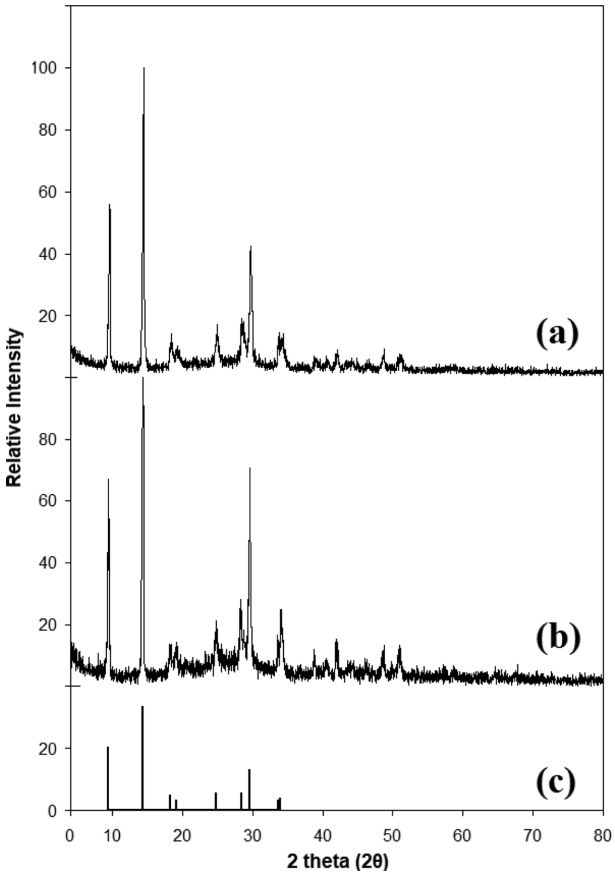

Fig. 10. Experimental powder X-ray diffraction (PXRD) pattern of (a) synthesized sample, and (b) used sample after five cycles, in comparison with a simulated PXRD pattern for $Mg_3(bdc)_3(H_2O)_2$ [18].

23-25,52]. These results may indicate the importance of the regeneration of the catalyst after the esterification reaction.

CONCLUSION

Nanosheets of magnesium-based MOF, $Mg_3(bdc)_3(H_2O)_2$, were synthesized via microwave irradiation and characterized with various techniques. The synthesized MOF was successfully utilized for the microwave-assisted production of biodiesel from esterification of oleic acid with methanol. Microwave irradiation was used as a power source for the esterification reaction, which caused a reduction in the reaction time. The results indicated that Mg-MOF catalyst showed high conversion percentage (97%) that followed pseudo-first order, under mild reaction conditions (MW power: 150 watts, reaction time: 8 min, molar ratio of oleic acid to methanol: 1 : 15 and catalyst amount 0.15 wt%). The catalyst showed re-usability feature for the esterification process.

SUPPORTING INFORMATION

Additional information as noted in the text. This information is available via the Internet at http://www.springer.com/chemistry/journal/11814.

REFERENCES

1. J. C. J. Bart, N. Palmeri and S. Cavallaro, *Biodiesel science and technology, 1st Ed., from soil to oil*, Woodhead Publishing Ltd (2010).
2. S. R. Sinsel, R. L. Riemke and V. H. Hoffmann, *Renew. Energy*, **145**, 2271 (2020).
3. H. M. Wee, W. H. Yang, C. W. Chou and M. V. Padilan, *Renew. Sust. Energy Rev.*, **16**, 5451 (2012).
4. E. A. Ateq, *Biodiesel viscosity and flash point determination*, Master's thesis, An-Najah National University, Nablus, Palestine (2015).
5. M. Cea, M. E. González, M. Abarzúa and R. Navia, *J. Environ. Manage.*, **242**, 171 (2019).
6. J. H. Lee, S. B. Kim, H. Y. Yoo, J. H. Lee, S. O. Han, C. Park and S. W. Kim, *Korean J. Chem. Eng.*, **30**, 1335 (2013).
7. L. Fjerbaek, V. Christensen and B. Norddahl, *Biotechnol. Bioeng.*, **102**, 1298 (2009).
8. Y. Yeşiloğlu, *Process Biochem.*, **40**, 2155 (2005).
9. A. S. Silitonga, H. H. Masjuki, T. M. I. Mahlia, H. C. Ong, A. E. Atabani and W. T. Chong, *Renew. Sust. Energy Rev.*, **24**, 514 (2013).
10. B. R. Vahid and M. Haghighi, *Energy Convers. Manage.*, **126**, 362 (2016).
11. M. Kim, C. DiMaggio, S. O. Salley and K. Y. S. Ng, *Bioresour. Technol.*, **118**, 37 (2012).
12. H. Wan, C. Chen, Z. Wu, Y. Que, Y. Feng, W. Wang, L. Wang, G. Guan and X. Liu, *ChemCatChem.*, **7**, 441 (2015).
13. B. Aghabarari and N. Dorostkar, *J. Taiwan Inst. Chem. Eng.*, **45**, 1468 (2014).
14. I. Istadi, D. D. Anggoro, L. Buchori, D. A. Rahmawati and D. Intaningrum, *Proc. Environ. Sci.*, **23**, 385 (2015).
15. S. Soltani, U. Rashid, R. Yunus and Y. H. Taufiq-Yap, *Fuel*, **178**, 253 (2016).
16. J. A. Kaduk, *Acta Cryst. Sec. B*, **58**, 815 (2002).
17. J. A. Rood, B. C. Noll and K. W. Henderson, *Main Group Chem.*, **5**, 21 (2006).
18. R. P. Davies, R. J. Less, P. D. Lickiss and A. J. P. White, *Dalton Trans.*, **24**, 2528 (2007).
19. C. A. Williams, A. J. Blake, C. Wilson, P. Hubberstey and M. Schröder, *Cryst. Growth Des.*, **8**, 911 (2008).
20. P. D. C. Dietzel, R. Blom and H. Fjellvåg, *Eur. J. Inorg. Chem.*, **23**, 3624 (2008).
21. S. Mendiratta, M. Usman, T. W. Tseng, T. T. Luo, S. F. Lee, L. Zhao, M. K. Wu, M. M. Lee, S. S. Sun, Y. C. Lin and K. L. Lu, *Eur. J. Inorg. Chem.*, **10**, 1669 (2015).
22. A. Biswas, M. B. Kim, S. Y. Kim, T. U. Yoon, S. I. Kim and Y. S. Bae, *RSC Adv.*, **6**, 81485 (2016).
23. Z. Hasan, J. W. Jun and S. H. Jhung, *Chem. Eng. J.*, **278**, 265 (2015).
24. A. Nikseresht, A. Daniyali, M. Ali-Mohammadi, A. Afzalinia and A. Mirzaie, *Ultrason. Sonochem.*, **37**, 203 (2017).
25. H. M. A. Hassan, M. A. Betiha, S. K. Mohamed, E. A. El-Sharkawy and E. A. Ahmed, *Appl. Surf. Sci.*, **412**, 394 (2017).
26. N. R. Khan and V. K. Rathod, *Process Biochem.*, **75**, 89 (2018).
27. R. K. Singh, R. Kumar, D. P. Singh, R. Savu and S. A. Moshkalev, *Mater. Today Chem.*, **12**, 282 (2019).
28. L. Y. Meng, B. Wang, M. G. Ma and K. L. Lin, *Mater. Today Chem.*, **1-2**, 63 (2016).
29. F. Mavandadi and Å. Pilotti, *Drug Discovery Today*, **11**, 165 (2006).
30. S. Chellappan, K. Aparna, C. Chingakham, V. Sajith and V. Nair, *Fuel*, **246**, 268 (2019).
31. A. Sharma, P. Kodgire, S. S. Kachhwaha, H. B. Raghavendra and K. Thakkar, *Mater. Today-Proc.*, **5**, 23064 (2018).
32. J. J. Lin and Y. W. Chen, *J. Taiwan Inst. Chem. E.*, **75**, 43 (2017).
33. L. A. Jermolovicius, L. C. M. Cantagesso, R. B. do Nascimento, E. R. de Castro, E. V. S. Pouzada and J. T. Senise, *Chem. Eng. Process*, **122**, 380 (2017).
34. S. A. El Sherbiny, A. A. Refaat and S. T. El Sheltawy, *J. Adv. Res.*, **1**, 309 (2010).
35. F. Ketzer, D. Celante and F. de Castilhos, *Micropor. Mesopor. Mater.*, **291**, 109704 (2020).
36. Y. T. Wang, Z. Fang and F. Zhang, *Catal. Today*, **319**, 172 (2019).
37. C. Cannilla, G. Bonura, F. Costa and F. Frusteri, *Appl. Catal. A*, **566**, 121 (2018).
38. Z. T. Alismaeel, A. S. Abbas, T. M. Albayati and A. M. Doyle, *Fuel*, **234**, 170 (2018).
39. A. Hykkerud and J. M. Marchetti, *Biomass Bioenergy*, **95**, 340 (2016).
40. H. M. Abd El Salam and T. Zaki, *Inorg. Chim. Acta*, **471**, 203 (2018).
41. Z. Zhou, L. Mei, C. Ma, F. Xu, J. Xiao, Q. Xia and Z. Li, *Chem. Eng. Sci.*, **147**, 109 (2016).
42. A. L. Cardoso, S. C. G. Neves and M. J. da Silva, *Energies*, **1**, 79 (2008).
43. O. Ilgen, *Fuel Process. Technol.*, **124**, 134 (2014).
44. P. Lv, J. Wang, S. Xing, Z. Li, P. Fan and Z. Wang, *Comparison between heterogeneous acid and base catalyzed biodiesel production: catalytic mechanism and performance*, 8th international symposium on acid base catalysis, 7-10 May 2017, Rio de Janeiro, Brazil.
45. A. M. El-Nahas, T. A. Salaheldin, T. Zaki, H. H. El-Maghrabi, A. M. Marie, S. M. Morsy and N. K. Allam, *Chem. Eng. J.*, **322**, 167 (2017).
46. S. Gan, H. K. Ng, P. H. Chan and F. L. Leong, *Fuel Process. Technol.*, **102**, 67 (2012).
47. J. G. Vitillo, *RSC Adv.*, **5**, 36192 (2015).
48. M. Shaban, M. R. Abukhadra, R. Hosny, A. M. Rabie, S. A. Ahmed and N. A. Negm, *J. Mol. Liq.*, **279**, 224 (2019).
49. F. G. Cirujano, A. Corma and F. X. Llabrés i Xamena, *Catal. Today*, **257**, 213 (2015).
50. R. Peña-Rodríguez, E. Márquez-López, A. Guerrero, L. E. Chiñas, D. F. Hernández-González and J. M. Rivera, *Mater Lett.*, **217**, 117 (2018).
51. M. Han, Y. Li, Z. Gu, H. Shi, C. Chen, Q. Wang, H. Wan and G. Guan, *Colloids Surf. A*, **553**, 593 (2018).
52. W. Xie and F. Wan, *Chem. Eng. J.*, **365**, 40 (2019).

Supporting Information

Microwave-assisted production of biodiesel using metal-organic framework $Mg_3(bdc)_3(H_2O)_2$

Howaida AbdelSalam[*], Heba Hassan El-Maghrbi[,†], Fouad Zahran[***,†], and Tamer Zaki[**,****]**

*Analysis and Evaluation Division, Egyptian Petroleum Research Institute, Nasr City, P. O. Box 11727, Cairo, Egypt
**Catalysis Department, Petroleum Refining Division, Egyptian Petroleum Research Institute, Nasr City, P. O. Box 11727, Cairo, Egypt
***Chemistry Department, Faculty of Science, Helwan University, 11795, Cairo, Egypt
****EPRI-Nanotechnology Center, Egyptian Petroleum Research Institute, Nasr City, P. O. Box 11727, Cairo, Egypt
(*Received 24 September 2019 • accepted 12 January 2020*)

IR, TGA and XRD Analysis for MOF before and after immersing in methanol

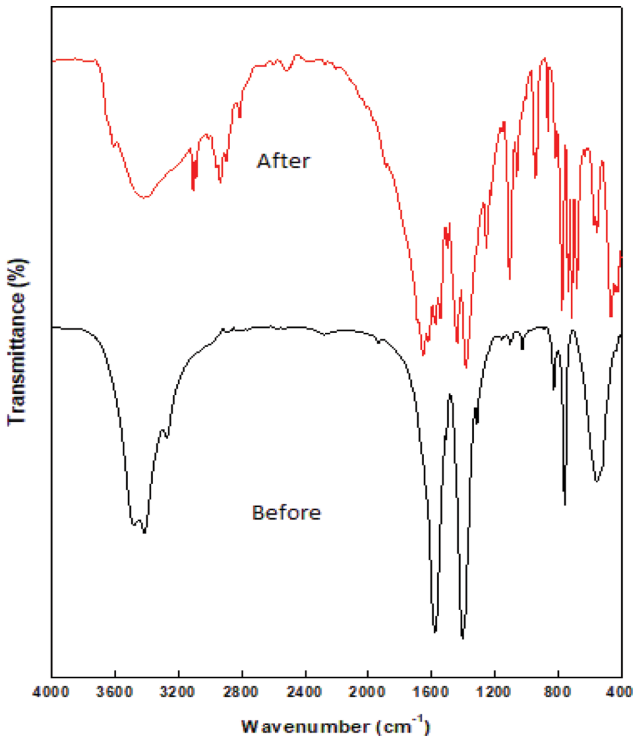

Fig. S1. IR spectra for MOF before and after immersing in methanol.

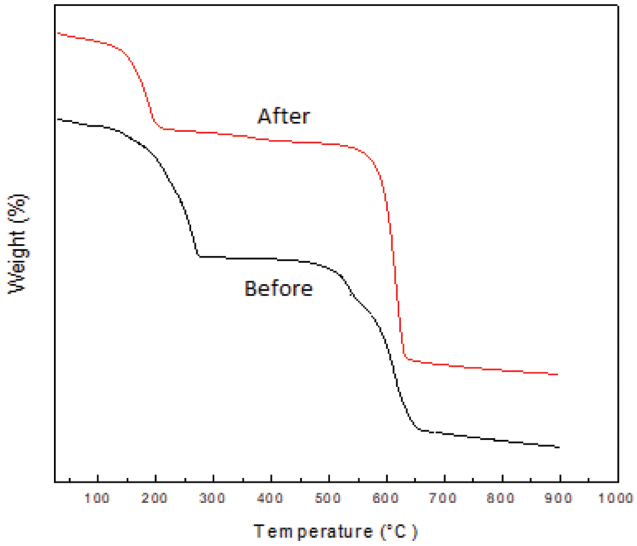

Fig. S2. TGA curves for MOF before and after immersing in methanol.

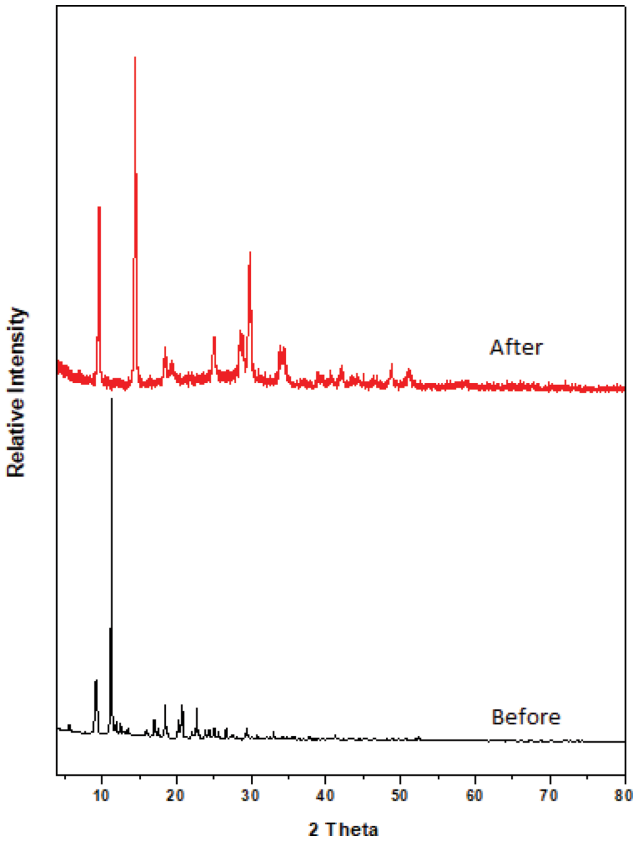

Fig. S3. XRD patterns for MOF before and after immersing in methanol.